Simple fabrication and characterization of discontinuous carbon fiber reinforced aluminum matrix composite for lightweight heat sink applications

Hiroki Kurita, Emilien Feuillet, Thomas Guillemet, Jean-Marc Heintz, Akira Kawasaki, Jean-François Silvain

Acta Metall. Sin. (Engl. Lett.), 2014

Simple Fabrication and Characterization of Discontinuous Carbon Fiber Reinforced Aluminum Matrix Composite for Lightweight Heat Sink Applications

Hiroki Kurita · Emilien Feuillet · Thomas Guillemet · Jean-Marc Heintz · Akira Kawasaki · Jean-François Silvain

Abstract The constant increase in power and heat flux densities encountered in electronic devices fuels a rising demand for lightweight heat sink materials with suitable thermal properties. In this study, discontinuous pitch-based carbon fiber reinforced aluminum matrix (Al-CF) composites with aluminum–silicon alloy (Al–Si) were fabricated through hot pressing. The small amount of Al–Si contributed to enhance the sintering process in order to achieve fully dense Al–CF composites. A thermal conductivity and CTE of 258 W/(m K) and 7.0×10^{-6}/K in the in-plane direction of the carbon fibers were obtained for a ($Al_{95\ vol\%}$ + $Al–Si_{5\ vol\%}$)-$CF_{50\ vol\%}$ composite. Carbon fiber provides the reducing of CTE while the conservation of thermal conductivity and weight of Al. The achieved CTEs satisfy the standard requirements for a heat sink material, which furthermore possess a specific thermal conductivity of 109 W cm^3/(m K g). This simple process allows the low-cost fabrication of Al–CF composite, which is applicable for a lightweight heat sink material.

KEY WORDS: Carbon fiber; Metal-matrix composites (MMCs); Thermal properties; Powder processing

1 Introduction

The continuous progress of active electronic components in terms of operating power, frequency, and miniaturization requires sophisticated heat sink materials demonstrating a high thermal conductivity and an adapted coefficient of thermal expansion (CTE) to mitigate thermal stresses in close vicinity to the semiconductors and ceramics substrates [1]. Composite materials have long been recognized as promising potential heat sink materials due to their tunable thermal properties. In such context, alloy reinforcements, e.g., nickel–iron (Ni–Fe), copper–tungsten (Cu–W), and copper–molybdenum (Cu–Mo) alloys are attractive due to their high thermal conductivities and low CTEs [1, 2]. Aluminum (Al) and copper (Cu) are common matrix materials due to their high thermal conductivities. Aluminum is superior as a matrix material for lightweight heat sink, not only because of its low density, but also due to its low price and low melting point. Therefore, Al-based composite materials have recently attracted much attention as a new generation of heat sink materials because of their promising combination of high thermal conductivity, low CTE, and low density.

One can find two main routes for Al-based composites sintering: liquid-state methods and solid-state methods. Liquid-phase methods (e.g., infiltration, stir casting) allow the easy densification of Al-based composites with high volume fractions of reinforcement and a small quantity of binder. However, this process is not valid when planning to

H. Kurita (✉)
DEN/DANS/DMN/SRMA/LTMEx, CEA Saclay, Gif-sur-Yvette, France
e-mail: hiroki.kurita@live.com

E. Feuillet · T. Guillemet · J.-M. Heintz · J.-F. Silvain
Institute of Condensed Matter Chemistry of Bordeaux, Bordeaux, France

A. Kawasaki
Department of Materials Processing, Graduate School of Engineering, Tohoku University, Sendai, Japan

fabricate Al-based composites with reinforcement that are reactive with Al [3]. Solid-phase methods (mostly relying on powder metallurgy) can enable the fabrication of Al-based composites with small internal reactivity. However, aluminum oxide (Al_2O_3) formation on aluminum particles often prevents the densification process from being optimal by mitigating interfacial reactivity, which is critical to enhance bonding at the Al matrix/reinforcement interface [4–6].

Numerous materials have been considered for reinforcing the Al matrix of Al-based heat sink composite materials. Among them, silicon carbides (SiC) are low cost and low CTE. The fabrication of SiC particle reinforced Al matrix composite materials with a thermal conductivity and CTE of 170–220 W/(m K) and (6.2–7.3) $\times$ 10^{-6}/K, respectively, has been demonstrated as possible [1]. However, SiC particles exhibit a strong drawback that it is unreactive with Al [1], and causes inhomogeneous mechanical and phase distribution [7]. Lai et al. [8] reported an improvement in the mechanical properties of an Al matrix through the addition of aluminum nitride (AlN) reinforcement to create Al–AlN composites. Despite the fact that AlN is not reactive with Al, AlN reinforcements show high thermal conductivity and Al–AlN composites tend to have good/interesting thermal properties.

Carbon fibers, among them in particular pitch-based carbon fibers, are also expected to be a promising lightweight (1.6–2.2 g/cm^3) reinforcement material for heat sink composites. The carbon fibers show anisotropic thermal properties, a medium to high thermal conductivity (100–900 W/(m K)) and a low CTE (-1.5 to -1.0 $\times$ 10^{-6}/K at room temperature) in the longitudinal direction, and a low thermal conductivity (5–10 W/(m K)) and a medium CTE (10.0–12.0 $\times$ 10^{-6}/K) in the transverse direction. The carbon fibers are used as both continuous and discontinuous reinforcement [2]. Continuous carbon fibers achieve higher thermal conductivity relative to discontinuous carbon fibers reinforced composites, although the final thermal properties must be anisotropic. Discontinuous carbon fibers reinforced composites have an advantage in the fabrication process over continuous fibers reinforced composites that their thermal properties are isotropic if discontinuous carbon fibers are randomly oriented.

The purpose of this study was the fabrication of discontinuous carbon fiber reinforced aluminum matrix (Al–CF) composites with light weight, low CTE, and high thermal conductivity. Conventional hot pressing was employed as the fabrication process in order to reduce the material processing costs. Due to its lower melting point relative to Al, aluminum–silicon alloy (Al–Si) [9] was considered an interesting liquid-phase material to help densify and consolidate the Al-CF composites. Thus, a small amount of Al–Si alloy powder was introduced in the powder mix to melt below the matrix melting point upon sintering.

2 Materials and Methods

2.1 Materials

Spherical Al powder (F3731, Hermillon Powders) with an average diameter of 8 μm and discontinuous pitch-based carbon fibers (Raheama® R-A301, Teijin Limited) with an average length of 200 μm and a thermal conductivity of 600 W/(m K) in the longitudinal direction were mixed together. Al-11.3Si (at.%) powder (F2071, Hermillon Powders) with a melting point of 584.6 °C was added to the mixture.

2.2 Fabrication Process

Discontinuous pitch-based carbon fibers and $Al_{95\ vol\%}$ + $Al–Si_{5\ vol\%}$ composite matrix powders were mixed for 5 min in air. The carbon fiber volume fraction of the final Al–CF composite was controlled to be 10, 20, 30, 40, and 50 vol%. Mixed composite powders were hot-pressed for 30 min at 600 °C (between the melting points of aluminum and Al–Si) under a uniaxial compressive stress of 60 MPa. The hot pressing temperature was monitored by a K-type thermocouple located at the center of the carbon mold.

2.3 Measurement

The relative density of the Al–CF composites was measured by the Archimede's principle. The thermal conductivity was calculated as the product of the density, heat capacity, and thermal diffusivity of Al–CF composites, which was measured by the flash laser method (NETZSCH LFA 457, MicroFlash®) at room temperature. Then, the thermal conductivity in directions parallel and perpendicular to the stress axis (transverse and in-plane directions of carbon fibers, respectively) was evaluated. The CTE was measured in the direction perpendicular to the stress axis in the hot press (i.e., the in-plane direction of the carbon fibers) under an argon gas flow in two thermal cycles between room temperature and 250 °C with 2 °C/min of heating/cooling rate by using a CTE measurement system (NETZSCH DIL 402, PC®). The CTEs were estimated from average values obtained between 100 and 180 °C.

Microstructural characterization of the Al-CF composite was carried out through scanning electron microscopy (SEM; Tescan, VEGA©) and high-resolution transmission electron microscopy (HR-TEM; JEOL 2,000-FX). Elemental analysis of the Al-CF composites was performed

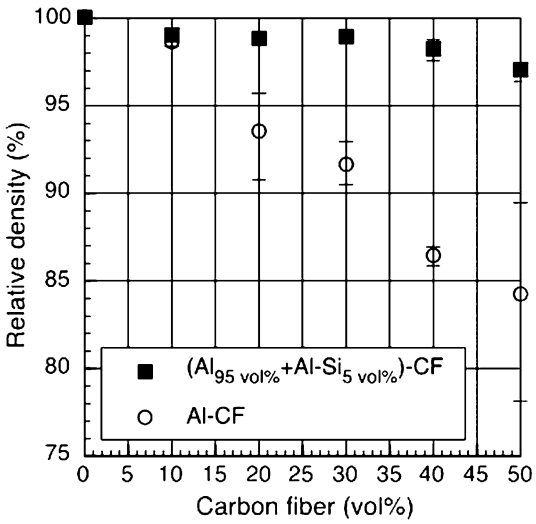

Fig. 1 Relative density of ($Al_{95\ vol\%}$ + Al–$Si_{5\ vol\%}$)– and Al–CF composites

through energy dispersive X-ray spectroscopy (EDS; the EDS detector attached SEM microscope) and electron probe microanalyzer (EPMA; CAMECA SX 100).

3 Results

3.1 Relative Density

Figure 1 shows the relative density of the ($Al_{95\ vol\%}$ + (Al–$Si)_{5\ vol\%}$)–CF and Al-CF composites. With less than 10 vol% of carbon fibers, the relative densities of ($Al_{95\ vol\%}$ + (Al–$Si)_{5\ vol\%}$)-CF and Al-CF composites were 99%. ($Al_{95\ vol\%}$ + (Al–$Si)_{5\ vol\%}$)–CF composites were shown to exhibit high levels of relative density up to 50 vol% of carbon fiber (e.g., 97% in ($Al_{95\ vol\%}$ + (Al–$Si)_{5\ vol\%}$)–$CF_{50\ vol\%}$ composite). In contrast, the relative density of the Al–CF composites was observed to drastically decrease with a large volume fraction of carbon fibers.

Figure 2 shows the SEM micrographs of densified ($Al_{95\ vol\%}$ + Al–$Si_{5\ vol\%}$)–CF and Al-CF composites. ($Al_{95\ vol\%}$ + Al–$Si_{5\ vol\%}$)–1CF composites exhibit a tight Al/CF interface, and the carbon fibers tended to be aligned in the in-plane direction due to the uniaxial compressive stress in the hot press [10]. However, the fiber orientation shows imperfections, and it seemed that a few inclination of the fibers existed (approximately ±25°) as shown in Fig. 2b. It was observed that the carbon fibers contacted each other and tangled in the Al matrix when the carbon fibers volume fraction exceeded 30 vol%, while the carbon fibers were individually and uniformly dispersed in the Al matrix with a carbon fiber volume fraction of less than 30 vol% (see Fig. 2c). As shown in Fig. 2d, the absence of Al–Si alloy led to the creation of voids at the interface between the Al matrix particles and the carbon fibers. Furthermore, it was observed no preferred carbon fibers orientation and the carbon fibers oriented in direction parallel to the stress axis of hot press (indicated as the white arrows in Fig. 2d) in the Al–CF composites due to the deficient densification of the composites.

Figure 3a shows the EPMA elemental mapping on ($Al_{95\ vol\%}$ + Al–$Si_{5\ vol\%}$)–$CF_{50\ vol\%}$ composite material. The bright parts in the three images indicate the presence of Al, C, and Si atoms, respectively. Indeed, Al matrix and the carbon fiber were showed as the bright parts in the EPMA elemental mapping of Al and C atoms. The EPMA elemental mapping of Si atom revealed that Si existed at the small spaces between the Al particle boundaries, carbon fibers, and Al/CF interface. Moreover, EDS analysis supported the result of EMPA electrical mapping as shown in Fig. 3b; the white areas (spot 3), which were filled up the slight spaces between Al matrix (spot 1) and carbon fiber (spot 2), were Al–Si.

3.2 Thermal Conductivity

Figure 4 shows the thermal conductivities of the Al + Al–Si matrix prepared by hot pressing with the same fabrication conditions as the composite materials. The thermal conductivity of $Al_{95\ vol\%}$ + Al–$Si_{5\ vol\%}$ matrix (197 W/(m K)) was slightly lower than the hot-pressed Al (202 W/(m K)) because of the lower thermal conductivity of Al–Si relative to pure Al.

Figure 5 shows the thermal conductivities of ($Al_{95\ vol\%}$ + Al–$Si_{5\ vol\%}$)–CF and Al-CF composites. The thermal conductivities of ($Al_{95\ vol\%}$ + Al–$Si_{5\ vol\%}$)–CF and Al–CF composites were observed to decrease with increasing the carbon fiber volume fraction in the transverse direction of the carbon fibers. In addition, the transverse thermal conductivity of Al-CF composites was shown to be low compared with that of the ($Al_{95\ vol\%}$ + Al–$Si_{5\ vol\%}$)–CF composites. In the in-plane direction of the carbon fiber, the thermal conductivity of ($Al_{95\ vol\%}$ + Al–$Si_{5\ vol\%}$)–CF composites was observed to increase with carbon fiber addition, and reached 258 W/(m K) for the ($Al_{95\ vol\%}$ + Al–$Si_{5\ vol\%}$)–$CF_{50\ vol\%}$ composites. This thermal conductivity value was slightly higher than that of pure Al. It indicated the thermal conductivity of Al was maintained despite the addition of carbon fiber. On the other hand, the in-plane thermal conductivity of Al–CF composites was determined to drastically decrease with the carbon fiber addition.

3.3 Coefficient of Thermal Expansion (CTE)

Figure 6 shows the CTEs obtained from ($Al_{95\ vol\%}$ + Al–$Si_{5\ vol\%}$)–CF and Al–CF composites in the carbon fibers in-plane direction. The CTE of the Al matrix (25.3×10^{-6}/K) was measured to be higher than that of pure Al

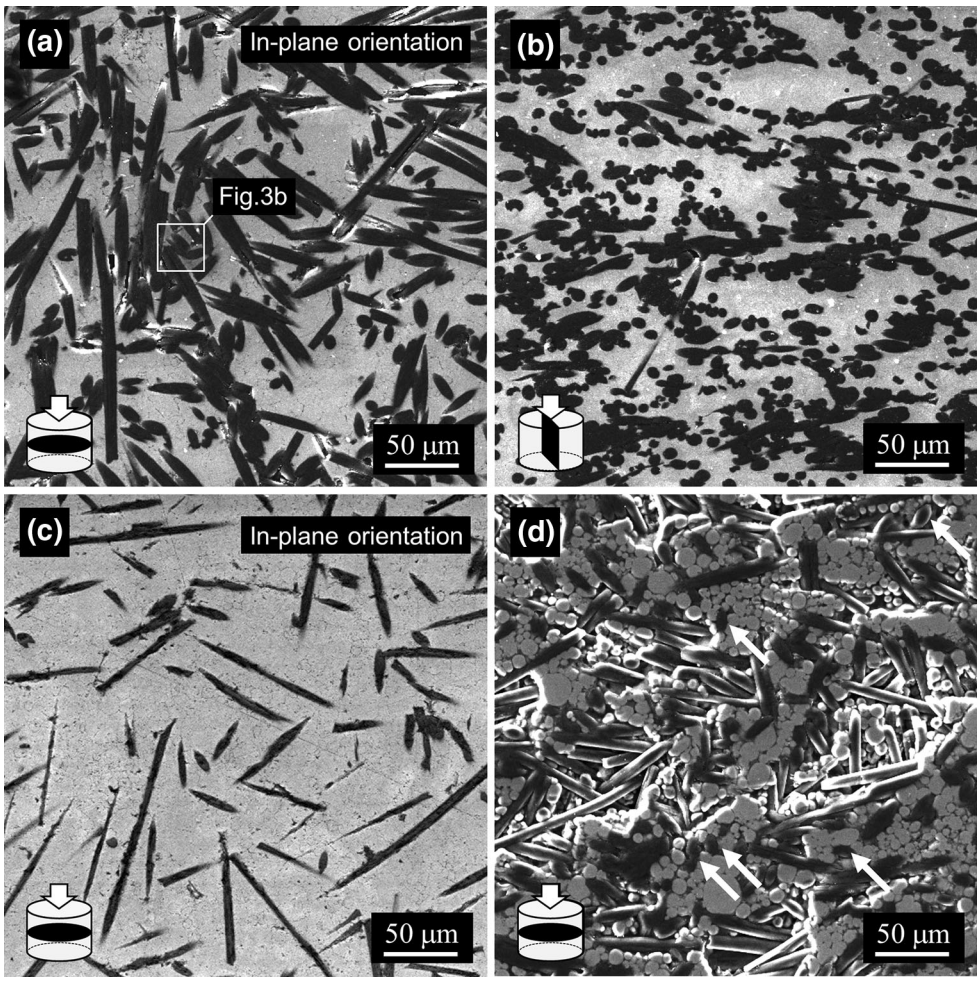

Fig. 2 SEM micrographs of ($Al_{95\ vol\%}$ + Al–$Si_{5\ vol\%}$)–$CF_{50\ vol\%}$ composite in the in-plane **a** and transverse directions **b** of the carbon fiber, **c** ($Al_{95\ vol\%}$ + Al–$Si_{5\ vol\%}$)–$CF_{20\ vol\%}$ composite in the in-plane direction of the carbon fiber, **d** Al–$CF_{50\ vol\%}$ composite in the in-plane direction of carbon fiber

(24.0×10^{-6}/K). The CTEs of ($Al_{95\ vol\%}$ + Al–$Si_{5\ vol\%}$)–CF and Al–CF composites decreased with the addition of up to a 20 vol% of the carbon fibers. However, the CTE of Al–$CF_{30\ vol\%}$ composite was measured to be higher than that of the Al-$CF_{20\ vol\%}$ composite. Furthermore, the CTE of the Al–$CF_{40\ vol\%}$ composite was non-measurable due to the deterioration in the composite, due to its low relative density. The CTE of the ($Al_{95\ vol\%}$ + Al-$Si_{5\ vol\%}$)–CF composites reached 7.0×10^{-6}/K with a 50% carbon fiber volume fraction. This result revealed that the addition of the carbon fiber achieved the drastic improvement in CTE of Al (24.0×10^{-6}/K). The CTEs were shown to be stable upon thermal cycling for both ($Al_{95\ vol\%}$ + Al–$Si_{5\ vol\%}$)–CF and Al–CF composites.

3.4 Microstructure Characterization

Figure 7 shows TEM micrographs of the Al/CF interface in a ($Al_{95\ vol\%}$ + Al–$Si_{5\ vol\%}$)–$CF_{50\ vol\%}$ composite material. Al/CF interface showed good integrity, without any interfacial delamination. Needle-like aluminum carbide (Al_4C_3) crystals were observed to form on the sidewall of the carbon fibers, following the carbon fiber orientation. At the tip end of carbon fiber, Al_4C_3 crystals were observed as clusters. The carbon fiber tips were covered with Al_4C_3 crystals.

4 Discussion

4.1 Densification of Al-CF Composite with 5 vol% of Al–Si Alloy

Through hot pressing at 600 °C (between the melting points of Al (660 °C) and Al–Si (584.6 °C)), Al–Si changes to the liquid phase and infiltrates between the aluminum particles and the carbon fibers at Al/CF interfaces (see Fig. 3). Consequently ($Al_{95\ vol\%}$ + Al–$Si_{5\ vol\%}$)–CF composites

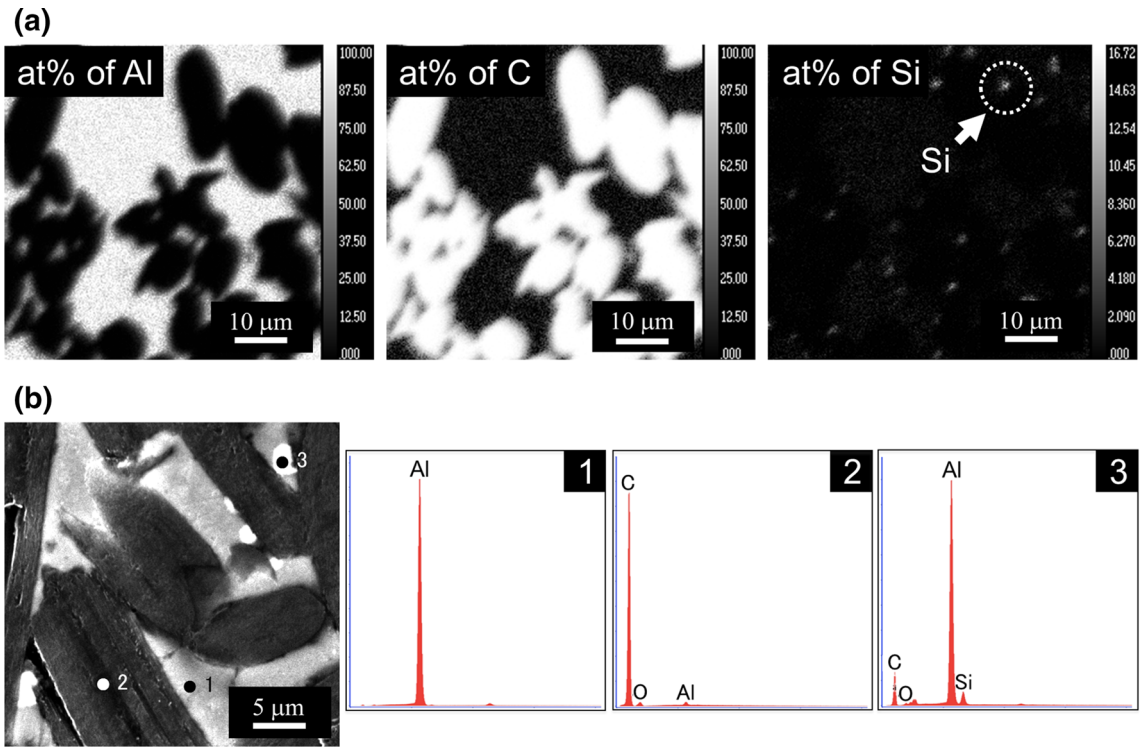

Fig. 3 Results of microanalysis: **a** EPMA mapping, **b** EDX spot scan in ($Al_{95\ vol\%}$ + Al–$Si_{5\ vol\%}$)–$CF_{50\ vol\%}$ composite

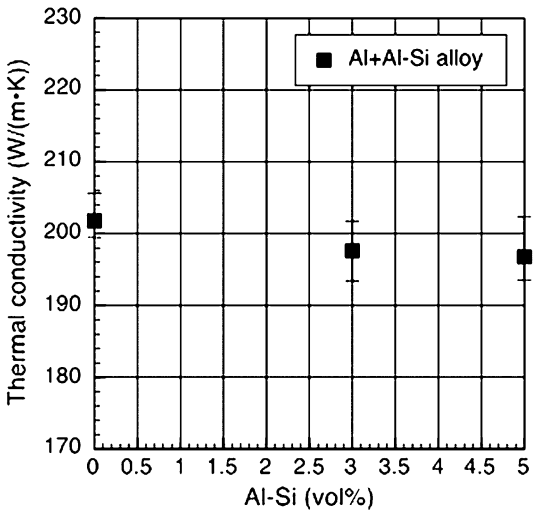

Fig. 4 Thermal conductivities of Al + Al–Si composites without the carbon fibers

maintain a high relative density (higher than 97% with 50 vol% of carbon fiber). This result clearly indicates that the small quantity of Al–Si added to the composite mixture effectively contributes to densify Al–CF composites, while slightly affects the thermal conductivity.

4.2 Thermal Conductivity

Carbon fibers have remarkable thermal conductivity in the longitudinal direction and lower thermal conductivity in the transverse direction [10, 11]. Therefore, the thermal conductivities of ($Al_{95\ vol\%}$ + Al–$Si_{5\ vol\%}$)–CF and Al–CF composites decrease with the carbon fiber addition in the transverse direction of the carbon fibers (see Fig. 5a). The lower thermal conductivities of Al–CF composites compared with that of ($Al_{95\ vol\%}$ + Al–$Si_{5\ vol\%}$)–CF composites indicate that the voids located at Al/CF interfaces interrupt effective heat transfer. On the other hand, in the in-plane direction of the carbon fibers, the thermal conductivity of ($Al_{95\ vol\%}$ + Al–$Si_{5\ vol\%}$)–CF composites increases, while the thermal conductivity of Al–CF composite decreases due to the low relative density.

We evaluated the applicability of the thermal conductivities experimentally obtained from ($Al_{95\ vol\%}$ + Al–$Si_{5\ vol\%}$)–CF composites. Nomura et al. [12] have suggested an equation to estimate the macro thermal conductivity, k, in short fibers reinforced composite as follows:

$$k_{11}^{*}(-)=\left\{\frac{f_f}{k_{f1}}+\frac{f_m}{k_m}-\frac{f_f f_m\left(\frac{1}{k_{f1}}-\frac{1}{k_m}\right)^2 h(\omega)}{\left(f_m-f_f\right)\left(\frac{1}{k_{f1}}-\frac{1}{k_m}\right)h(\omega)+\frac{f_f}{k_{f1}}+\frac{f_m}{k_m}}\right\}^{-1}, \quad (1)$$

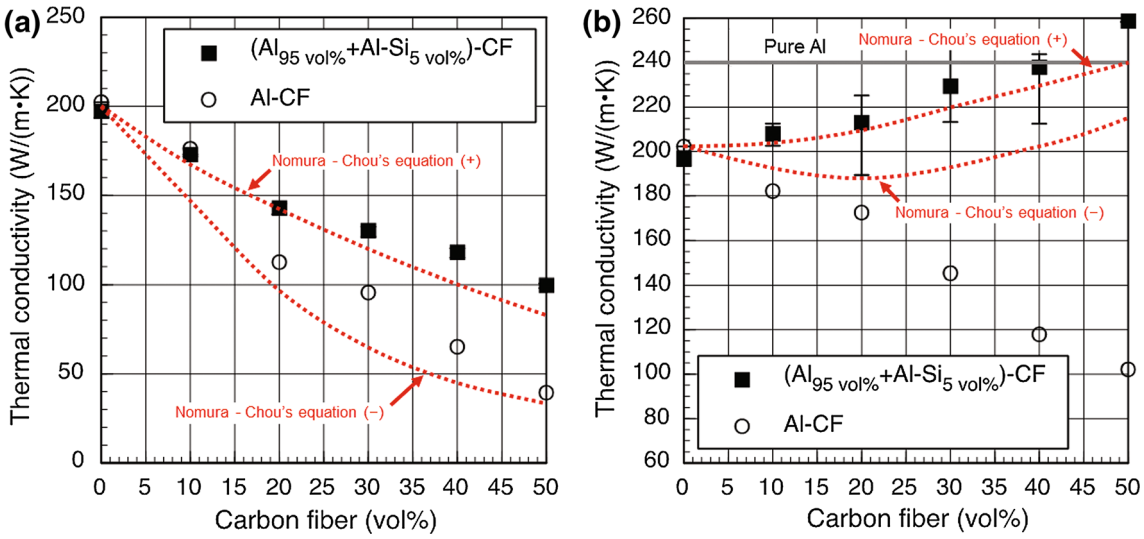

Fig. 5 Thermal conductivities of ($Al_{95\ vol\%}$ + Al–$Si_{5\ vol\%}$)– and Al–CF composites in the transverse direction **a** and in-plane direction **b** of the carbon fibers

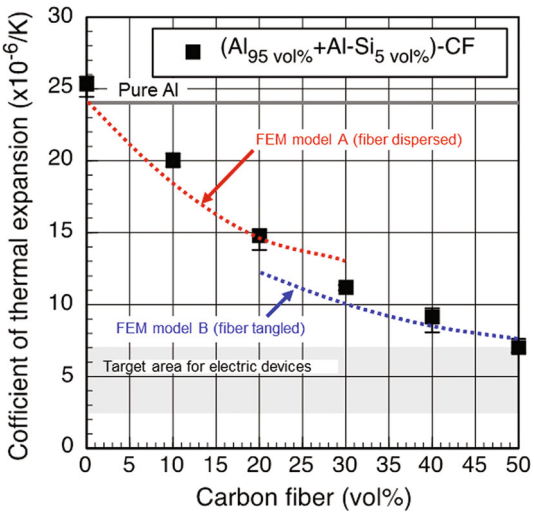

Fig. 6 CTEs of ($Al_{95\ vol\%}$ + Al-$Si_{5\ vol\%}$)– and Al–CF composites in the in-plane direction of the carbon fibers

$$k_{11}^{*}(+) = f_f k_{f1} + f_m k_m - \frac{f_f f_m \left(k_{f1} - k_m\right)^2 \{1 - h(\omega)\}}{\left(f_m - f_f\right)\left(k_{f1} - k_m\right)\{1 - h(\omega)\} + f_f k_{f1} + f_m k_m}, \tag{2}$$

$$k_{22}^{*}(-) = \left\{ \frac{f_f}{k_{f2}} + \frac{f_m}{k_m} - \frac{f_f f_m \left(\frac{1}{k_{f2}} - \frac{1}{k_m}\right)^2 \left\{1 - \frac{h(\omega)}{2}\right\}}{\left(f_m - f_f\right)\left(\frac{1}{k_{f2}} - \frac{1}{k_m}\right)\left\{1 - \frac{h(\omega)}{2}\right\} + \left(\frac{f_f}{k_{f2}} + \frac{f_m}{k_m}\right)} \right\}^{-1}, \tag{3}$$

$$k_{22}^{*}(+) = f_f k_{f2} + f_m k_m - \frac{f_f f_m \left(k_{f2} - k_m\right)^2 h(\omega)}{\left(f_m - f_f\right)\left(k_{f2} - k_m\right)h(\omega) + 2\left(f_f k_{f2} + f_m k_m\right)}, \tag{4}$$

in which,

$$h(\omega) = \frac{\omega^2}{\omega^2 - 1}\left[1 - \frac{1}{2}\left\{\left(\sqrt{\frac{\omega^2}{\omega^2 - 1}} - \sqrt{\frac{\omega^2 - 1}{\omega^2}}\right) \times \ln\left(\frac{\omega + \sqrt{\omega^2 - 1}}{\omega - \sqrt{\omega^2 - 1}}\right)\right\}\right]. \tag{5}$$

Nomura–Chou's equation provides estimations of upper (+) and lower (–) limits of the thermal conductivity. k_{11} and k_{22} stand for the thermal conductivities in the longitudinal and transverse directions, respectively; if short fibers are aligned in a similar direction, k_{22} equals k_{33}. f and k correspond to the volume fraction and the thermal conductivity, respectively, and the f and m subscripts stand for the fiber and matrix, respectively. ω is the aspect ratio of fiber reinforcement. In this study, the thermal conductivity of the aluminum matrix (k_m) is 240 W/(m K), and the thermal conductivity of the carbon fibers in the longitudinal direction (k_{f1}) and transverse direction (k_{f2}) are 600 and 10 W/(m K), respectively. ω is calculated from the length and diameter of the carbon fibers and is equal to 25. The thermal conductivities of ($Al_{95\ vol\%}$ + Al–$Si_{5\ vol\%}$)–CF composites are estimated from the average value of k_{11} and k_{22} (in the in-plane direction of the carbon fiber), and k_{22} (in the transverse direction of the carbon fiber). However, it should be taken into account that this estimation cannot discuss the thermal

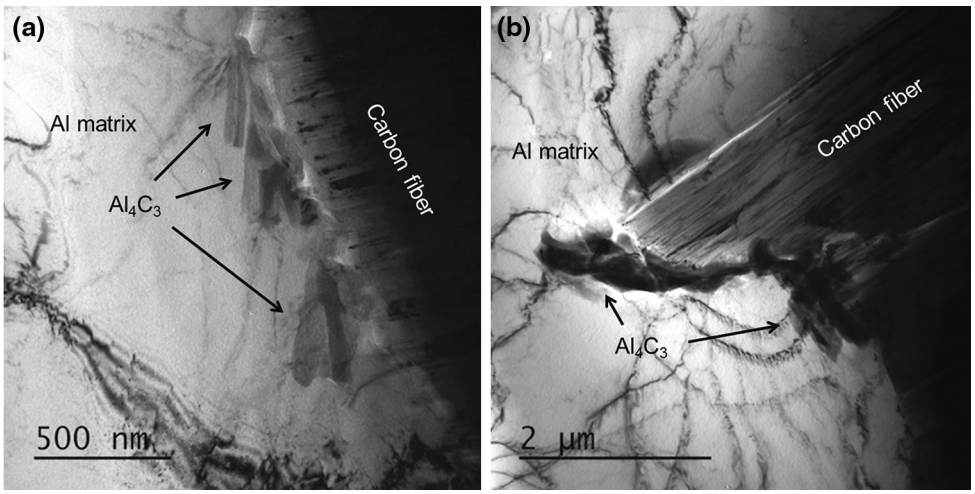

Fig. 7 TEM micrographs of ($Al_{95\ vol\%}$ + Al–$Si_{5\ vol\%}$)–$CF_{50\ vol\%}$ composite: **a** Al/CF interface, **b** tip of the carbon fiber

conductivities of Al–CF composite because there is no preferred carbon fibers orientation in Al–CF composite.

A comparison between the experimental and estimated thermal conductivities of ($Al_{95\ vol\%}$ + Al–$Si_{5\ vol\%}$)–CF composites are shown in Fig. 5. The experimental thermal conductivities of ($Al_{95\ vol\%}$ + Al–$Si_{5\ vol\%}$)–CF composites match the estimated theoretical upper limit of thermal conductivity with a carbon fiber volume fraction up to 30%. This result implies that the essential thermal conductivity of the carbon fiber is brought out in the Al + Al–Si matrix. In contrast, the thermal conductivities of the ($Al_{95\ vol\%}$ + Al–$Si_{5\ vol\%}$)–CF composite exceeded the estimated theoretical upper limit of thermal conductivity with a carbon fibers volume fraction over 30%. Nomura–Chou's equation does not take into account the fiber contacts and tangles observed in the SEM images for volume fractions higher than 30% (see Fig. 2). Therefore, it is inferred from the results that the direct contact of the carbon fibers has a positive influence and increases thermal conductivity. It is also assumed in Nomura–Chou's equation that the matrix/reinforcement interface exhibits strong bonding. In this study, ($Al_{95\ vol\%}$ + Al–$Si_{5\ vol\%}$)–CF composites have been shown to feature Al_4C_3 crystals at the Al/CF interface (see Fig. 7). Therefore, it seems that Al_4C_3 crystals promote effective heat transfer from the aluminum matrix to the carbon fibers through the Al–C chemical bonds.

4.3 Coefficient of Thermal Expansion (CTE)

Electronic packages are generally composed of multiple materials, such as semi-conductive components made of silicon or gallium arsenide, and ceramic substrates made of alumina, beryllia, and aluminum nitride [2, 13, 14]. To limit thermal stresses in the package, the heat sink material

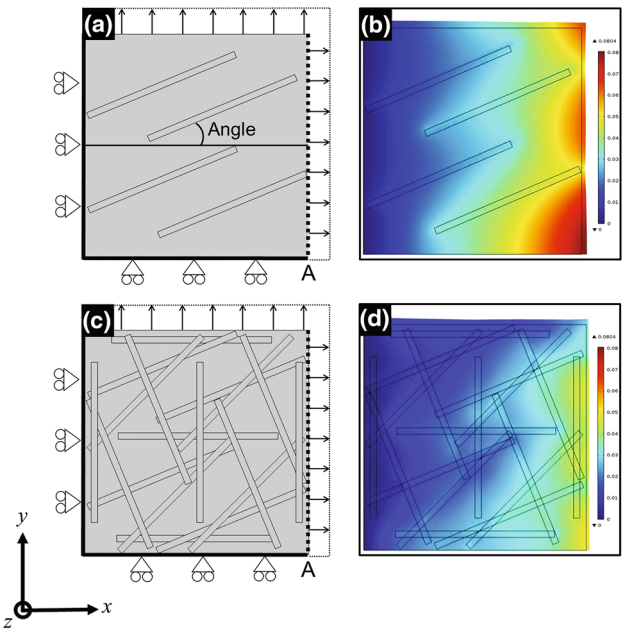

Fig. 8 FEM calculation images: **a** calculation criteria, **b** the displacement after calculation of ($Al_{95\ vol\%}$ + Al–$Si_{5\ vol\%}$)–$CF_{10\ vol\%}$ composite without the tangles of carbon fibers, **c** calculation criteria, **d** displacement after calculation of ($Al_{95\ vol\%}$ + Al–$Si_{5\ vol\%}$)–$CF_{50\ vol\%}$ composite with tangles of carbon fibers

should exhibit the CTE close to that of the surrounding layers, typically located around (2.6–7.0) × 10^{-6}/K. Our ($Al_{95\ vol\%}$ + Al–$Si_{5\ vol\%}$)–$CF_{50\ vol\%}$ composite shows a 7.0 × 10^{-6}/K of CTE, and thus can be applied as a heat sink material in electronic packages.

The applicability of experimental CTEs was evaluated. It has been previously reported that CTE does not follow the rule of mixtures due to interfacial thermal stress [15]. The CTE of continuous fiber reinforced composite follows several equations [16, 17], however, the CTE of

discontinuous fiber reinforced composites does not adhere because of its complex behavior.

A finite element method (FEM) calculation was carried out for the estimation of the CTEs of the ($Al_{95\ vol\%}$ + Al–$Si_{5\ vol\%}$)–CF composite. In this study, we prepared two types 2D-FEM model to calculate CTEs without carbon fiber contact (model A: to calculate CTEs of composites with carbon fibers volume fractions less than 30%) and with the carbon fiber contacts (model B: to calculate CTEs of composites with the carbon fibers volume fractions higher than 30%) as shown in Fig. 8a, c. The left and bottom sides on this FEM model were fixed in the *x* and *y* directions, respectively, in order to allow thermal expansion in the positive directions. The carbon fibers were fixed at the contact points between the carbon fibers in model B. In model A, the theoretical CTEs were estimated from the average displacements of the broken line A (in the *x* direction) for each fiber angle (0°, 22.5°, 45°, 67.5°, 90°). The volume fraction of the carbon fiber was controlled by the number of the carbon fibers. Figure 8b and d shows the values of displacement in the *x* direction and the deformation (ten times magnification) of the ($Al_{95\ vol\%}$ + Al–$Si_{5\ vol\%}$)–CF composite caused by dilation at 150 °C.

The comparison between the experimental and estimated CTEs of ($Al_{95\ vol\%}$ + Al–$Si_{5\ vol\%}$)–CF composites is shown in Fig. 6. The CTEs estimated by FEM model B are smaller than those determined by FEM model A, this calculation shows that the tangles of the carbon fiber contribute to further improve CTE in ($Al_{95\ vol\%}$ + Al–$Si_{5\ vol\%}$)–CF composites. The experimental CTEs of ($Al_{95\ vol\%}$ + Al–$Si_{5\ vol\%}$)–CF composites are consistent with the estimation by 2D-FEM calculation models, it seems that the remarkable CTE of the carbon fiber has been brought out in the Al matrix.

As mentioned above, hot pressing gives a inclination (±25°) of the carbon fibers in the ($Al_{95\ vol\%}$ + Al–$Si_{5\ vol\%}$)–CF composite. In order to investigate the influence on CTEs caused by the carbon fiber inclination, the CTEs on the *z*-*x* plane (*z* axis is the direction parallel to the stress axis in the hot press) were also estimated with the inclination (±25°) of the carbon fibers by using these FEM calculation models. The amount of CTE changes caused by the carbon fiber inclination is estimated as $+1.2 \times 10^{-6}$/K, therefore, it seems that the inclination (±25°) of the carbon fibers does not occur the drastic decrease in the CTEs of ($Al_{95\ vol\%}$ + Al–$Si_{5\ vol\%}$)–CF composites.

The CTEs were demonstrated to be stable, at least during two thermal cycles. This suggests that Al_4C_3 formation (Al–C chemical bond) enhance bonding at the Al/CF interface and contributes to thermal stability [18]. However, there is the potential for a decrease in the CTEs of ($Al_{95\ vol\%}$ + Al–$Si_{5\ vol\%}$)–CF composites in further thermal cycles [19].

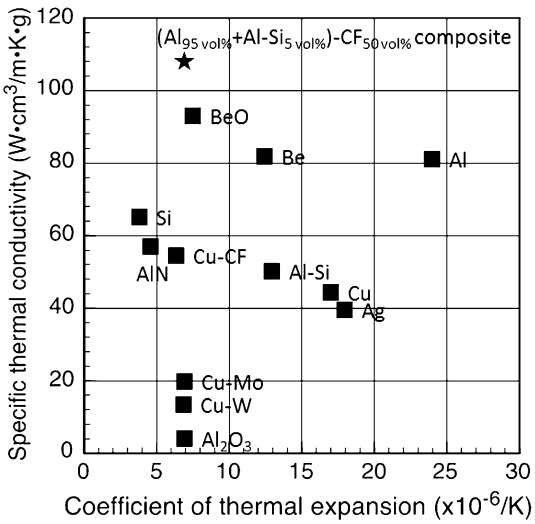

Fig. 9 Specific thermal conductivities versus CTE of several materials selected as heat sink materials

4.4 Specific Thermal Conductivity

Copper has a higher thermal conductivity (400 W/(m K)) and a lower CTE (17.0×10^{-6}/K) in relation to aluminum (240 W/(m K) in thermal conductivity and 24.0×10^{-6}/K in CTE). The fabrication of the carbon fiber reinforced copper (Cu–CF) composites with an improved CTE and thermal conductivity has been reported [2, 20–22]. However, the specific thermal conductivity (thermal conductivity per unit volume) recently attracted attention due to the heightened demand for lightweight heat sink materials. Figure 9 shows the specific thermal conductivity with respect to CTE of several materials potentially usable as heat sinks. The ($Al_{95\ vol\%}$ + Al–$Si_{5\ vol\%}$)–$CF_{50\ vol\%}$ composite fabricated in this study has a remarkable specific thermal conductivity (109 W cm^3/(m K g)) compared with other materials. Therefore, it seems that the ($Al_{95\ vol\%}$ + Al–$Si_{5\ vol\%}$)–$CF_{50\ vol\%}$ composite is a promising lightweight heat sink.

5 Conclusions

Al–CF composite materials were fabricated through conventional hot pressing with 5 vol% of Al–Si. The liquid phase of Al–Si infiltrated the composites and contributed to fabricate fully dense composite materials. The simple process developed in this study can help reduce the fabrication costs of Al–CF composite materials.

($Al_{95\ vol\%}$ + Al–$Si_{5\ vol\%}$)–$CF_{50\ vol\%}$ composite was shown to exhibit a thermal conductivity of 258 W/(m K) and a CTE of 7.0×10^{-6}/K in the in-plane direction of the carbon fibers, which satisfies the typical requirements for

heat sink materials, i.e., it was revealed that the addition of the carbon fiber provided the improvement in CTE of Al, while maintaining of thermal conductivity and light weight of Al. It is likely that interfacial Al_4C_3 crystal formation enhances the Al/CF interfacial bond, thus promoting effective heat transfer and thermal stability. Finally, the carbon fiber contacts and tangles are understood to further improve the thermal and thermomechanical properties of the materials.

The $(Al_{95\ vol\%} + Al–Si_{5\ vol\%})–CF_{50\ vol\%}$ composite developed in this study has a remarkable specific thermal conductivity (109 W cm^3/(m K g)) and is applicable as a lightweight heat sink for various electronic packages.

References

[1] D.D.L. Chung, Appl. Therm. Eng. **21**, 1593 (2001)
[2] C. Zweben, JOM **50**, 47 (1998)
[3] S. Lai, D.D.L. Chung, J. Mater. Sci. **29**, 3128 (1994)
[4] G. Latet, H. Kurita, T. Miyazaki, A. Kawasaki, J.F. Silvain, J. Mater. Sci. **49**, 3268 (2014)
[5] H. Kurita, H. Kwon, M. Estili, A. Kawasaki, Mater. Trans. **52**, 1960 (2011)
[6] H. Kwon, H. Kurita, M. Leparoux, A. Kawasaki, J. Nanosci. Nanotechnol. **11**, 4119 (2011)
[7] S. Lai, D.D.L. Chung, J. Mater. Sci. **29**, 2998 (1994)
[8] S. Lai, D.D.L. Chung, J. Mater. Sci. **29**, 6181 (1994)
[9] J.L. Murray, A.J. McAlister, Bull. Alloy Phase Diagr. **5**(1), 74 (1984)
[10] A. Veillère, J.M. Heintz, N. Chandra, J. Douin, M. Lahaye, G. Lalet, C. Vincent, J.F. Silvain, Mater. Res. Bull. **47**, 375 (2012)
[11] M.W. Pilling, B. Yates, M.A. Black, P. Tattersall, J. Mater. Sci. **14**, 1326 (1979)
[12] S. Nomura, T.W. Chou, J. Comput. Mater. **14**, 120 (1980)
[13] C. Zweben, in *Encyclopedia of Materials: Science and Technology*, ed. by K.H.J. Buschow, R. Cahn, M. Flemings, B. Ilschner, E. Kramer, S. Mahajan, P. Veyssiere (Elsevier Science, Oxford, 2001) p. 2676
[14] T. Ueno, T. Yoshioka, J. Ogawa, N. Ozoe, K. Sato, K. Yoshino, Synth. Met. **159**, 2170 (2009)
[15] Z.H. Karadeniz, D. Kumlutas, Compos. Stru. **78**, 1 (2007)
[16] R.A. Scharepy, J. Compos. Mater. **2**, 380 (1968)
[17] E. Sideridis, Compos. Sci. Technol. **51**, 301 (1994)
[18] G. Lalet, H. Kurita, T. Miyazaki, A. Kawasaki, J.F. Silvain, Mater. Lett. **130**, 32 (2014)
[19] G. Latet, H. Kurita, J.M. Heintz, G. Lacombe, A. Kawasaki, J.F. Silvain, J. Mater. Sci. **49**, 397 (2014)
[20] T. Guillemet, P.-M. Geffroy, J.M. Heintz, N. Chandra, Y. Lu, J.F. Silvain, Compos. Part A **43**(10), 1746 (2012)
[21] T. Schubert, B. Trindade, T. Weiβgärber, B. Kieback, Mater. Sci. Eng. A **475**, 39 (2008)
[22] K. Hanada, K. Matsuzaki, T. Sano, J. Mater. Process. Technol. **153–154**, 514 (2004)